scientific reports

Check for updates

OPEN

Toxic effects of biodegradable polylactic acid nanoplastics on developing zebrafish (*Danio rerio*)

F. Scalia[1,2,9], F. Capparucci[3,9], M. D. Amico[1], M. Marino[4], E. P. Lamparelli[4], L. Longhitano[5], S. Giallongo[2], R. Falleti[3], F. Rappa[1], C. Iaria[3], F. Marino[3], G. Della Porta[4,6], A. Marino Gammazza[7], F. Bucchieri[1], A. Santoro[4,6,10], F. Cappello[1,10] & M. A. Szychlinska[8,10]✉

Plastic contamination represents a significant threat to the environment with potential health risks for all species. Recently, bio-based plastics have been introduced as a green alternative to fossil-based ones. However, bioplastic degradation products present potentially harmful effects comparable to the fossil-based ones. Polylactic acid (PLA) is one of the most widely used bioplastics in the world and it requires high temperatures found in industrial composting, to degrade fully. These conditions are not typical of natural environments, where PLA degradation leads to the accumulation of micro- and nanoplastics. According to this finding, the aim of the present study was to assess PLA nanoplastics (PLA-NPs) potential harmful biological effects. PLA-NPs exposure effects have been assessed through the in vivo study on early-stage zebrafish bioaccumulation, cellular stress induction, and morpho-physiology, and through the in vitro study on HDF, used to mimic one of the modes of contamination route in humans, to evaluate their cellular uptake potential. For this purpose, zebrafish embryos were exposed to fluorescent PLA-NPs at the concentrations of 0.1 and 1 mg/L, up to 5 days. In the study, the parallel experiments were conducted by exposing zebrafish embryos to polystyrene MPs (PS-MPs), used as a well-established harmful positive control. No alterations in the Zebrafish Embryo Acute Toxicity Test parameters were found; however, heartbeat rate alteration in the PLA-NPs-treated zebrafish at 96 and 120 hpf have been observed. No remarkable morphological alterations of brain and liver tissue have been detected. The bioaccumulation of PLA-NPs was detectable at 72 and 96 hpf, presumably in the gastrointestinal tract. The gene expression analysis of cellular stress markers (*hmox1*, *nos2*, *sod1*, *sod2*, *il1β*, *tnfα*, *il4*, *il13*, *infγ*, *tbx21)* showed inflammation and oxidative stress induction in zebrafish at 72 and 120 hpf. Finally, HDF demonstrated uptake potential, suggesting their ability to bypass the dermal human barrier. The obtained results, accompanied by those on the exposure of developing zebrafish, and HDF cells, to the same concentrations of PS-MPs, raise concerns about the biological impact of PLA-based bioplastics and their use as a safe alternative to petroleum-based plastics.

Keywords Polylactic acid nanoplastics, Polystyrene microplastics, Developmental toxicity, Zebrafish, Human dermal fibroblasts

Plastic pollution represents a massive threat to the entire Earth's environment. Due to their resistance and durability, plastics find widespread use in the creation of daily-use objects, in packaging, transport, agriculture and the medical field, bringing global plastic production to over 400 million tons in 2023[1]. However, these

[1]Department of Biomedicine, Neuroscience and Advanced Diagnostics (BIND), University of Palermo, 90127 Palermo, Italy. [2]Department of Medicine and Surgery, University Kore of Enna, 94100 Enna, Italy. [3]Institute Slavko Bambir, Department of Chemical, Biological, Pharmaceutical and Environmental Sciences, University of Messina, 98166 Messina, Italy. [4]Department of Medicine, Surgery and Dentistry, University of Salerno, 84081 Baronissi, Italy. [5]Department of Biomedical and Biotecnological Sciences (BIOMETEC), University of Catania, 95100 Catania, Italy. [6]Interdepartmental Research Center for Biomaterials (BIONA), University of Salerno, 84084 Fisciano, Italy. [7]Department of Biological, Chemical and Pharmaceutical Sciences and Technologies (STEBICEF), University of Palermo, 90128 Palermo, Italy. [8]Department of Precision Medicine in Medical, Surgical and Critical Care (MEPRECC), University of Palermo, Via del Vespro N. 129, 90127 Palermo, Italy. [9]F. Scalia and F. Capparucci contributed equally to this work. [10]These authors jointly supervised this work: A. Santoro, F. Cappello and M. A. Szychlinska. ✉email: martaanna.szychlinska@unipa.it

features, together with a low level of plastics' disposal, result in the permanence and accumulation of plastic in the environment[2], especially the marine one, where plastic represents 80% of all waste[3]. Once in the sea, plastic is subject to atmospheric agents, determining its fragmentation, up to the formation of microplastics (MPs), with dimensions comprised between 1 µm and 5 mm, and nanoplastics (NPs) with dimensions from 1 nm to 1 µm[4].

Among standard petroleum-based plastics, polystyrene (PS) is one of the most common polymers used in numerous industries. PS exposed to UV rays rapidly forms MPs and NPs through fragmentation[5]. In this form, they can be assimilated by different aquatic organisms, leading to toxicity and organ damage, which can extend to human health through the food chain[6]. The bioaccumulation and ecotoxicological effects of PS-MPs have been widely demonstrated in several aquatic organisms[7]. In particular, exposure of zebrafish (*Danio rerio*) to PS-MPs was shown in several studies to cause inflammation, oxidative stress, alterations of lipid and energy metabolism, inducing toxicity at all tissue levels, as discussed in the review paper by Baghat et al.[8].

To tackle plastic pollution and safeguard the environment and living organisms, including humans, several policies have been adopted, such as banning single-use plastic items[9,10]. An important action in this regard is the use of "biodegradable" plastics as an alternative to petroleum-based ones. One of the most used bioplastics is Polylactic acid (PLA), a plant-based polymer, representing 33% of bioplastics produced in 2021[11]. Based on its biodegradable characteristics, PLA has found immediate application in agriculture, medical devices and food packaging[12]. However, the PLA-based product's disposal within the aquatic environment submits PLA to sub-optimal conditions, which leads to changes in its degradation rate[1,13]. Studies conducted in freshwater and seawater, under natural conditions in mesocosms, highlight that PLA and its copolymers show degradation in an aquatic environment, which is similar to that of synthetic plastics, leading to the formation of MPs and NPs[14,15]. The alarming stability of the PLA in the sea led to the necessity of investigating its effects on marine biota. Based on the few studies conducted on a limited number of aquatic species, PLA would be as toxic as petroleum-based plastics[16–18].

While a plethora of studies have investigated the effects of the ingestion and bioaccumulation of petroleum-based MPs in various species of fish, the studies investigating the effects of PLA-MPs and even more of PLA-NPs on fish remain limited, with few of them conducted on zebrafish. In these studies, the PLA-MPs demonstrated bioaccumulation in the liver, brain, and gills, behavioral changes, and alterations in pigmentation[19]. De Oliveira et al., observed a decrease in swimming speed and distance[20]. The skeletal development impairment was also observed in the study by Zhang et al., which further highlighted a greater toxicity of degraded PLA-MPs compared to the whole polymer[21]. Curiously, Duan et al., compared the bioaccumulation and toxicity of PLA-MPs and those of petroleum-based microplastics of poly(ethylene) (PE), on zebrafish, observing a dietary preference for PLA-MPs, which, in turn, induced damage of the intestinal tract and alteration of microbiota[22]. In only one study, up to date, the effects of PLA-NPs of 80 nm have been assessed in developing zebrafish, suggesting high immune-toxicity[23].

PLA, marketed as an eco-green alternative to conventional petroleum-based plastics, disappointed expectations by proving to be non-degradable in water and toxic to aquatic organisms. Further studies are necessary to understand the eco-toxicological effects of PLA-MPs and NPs on aquatic biota and human health. For this reason, the present study evaluates the effects of PLA-NPs of heterogeneous nanometric diameter (275 ± 75 nm) at the concentrations of 0.1-1 mg/L on developing zebrafish bioaccumulation, cellular stress, and morpho-physiological alteration induction, up to 120 hpf. Moreover, it investigates the PLA-NPs' capacity to cross the human dermal fibroblast (HDF) cell membrane. The concentrations of 0.1 and 1 mg/L of both plastics used in the study are considered environmentally relevant, as indicated elsewhere[24]. Moreover, a heterogeneous size population of PLA-NPs (275 ± 75 nm) was used to reproduce a more realistic condition of the presence of PLA degradation derivatives in the aquatic environment. Our results showed that our PLA-NPs treatment condition had no direct effects on the developmental parameters analyzed. However, we assessed an alteration in heartbeat rate of treated zebrafish, suggesting that PLA-NPs may indirectly impact heart function. Moreover, PLA-NPs demonstrated bioaccumulation potential already at 72 hpf related to alteration of gene expression levels of cellular stress markers. Furthermore, the results of in vitro study showed that PLA-NPs may cross the membrane of one of the most abundant human cell types, HDF. The results of the study were interpreted based on the results obtained from the parallel experiment conducted, exposing the developing zebrafish and HDF cells, to the same concentrations (0.1 and 1 mg/L) of PS-MPs.

Polystyrene is a widely used petroleum-based plastic product and a significant source of microplastic pollution. In recent years, its association with toxic effects has been frequently reported in scientific literature, providing a strong baseline for understanding the harmful impact of microplastics[25,26]. The goal of the present study was not merely to evaluate the toxicity of polylactic acid broadly, but to challenge the belief that biodegradable plastics like PLA are a safer and more sustainable option than traditional plastics. Thus, PS-MPs were used here as a positive control of toxicity induction and to validate the sensitivity and reliability of the experiment.

Materials and methods

Rhodamine-labelled polylactic acid nanoplastics (PLA-NPs)

PLA-NPs production: Microfluidics-assisted nanoprecipitation procedure

PLA-NPs were obtained by a microfluidics-assisted nanoprecipitation procedure. Briefly, Polylactic Acid (PLA) (Resomer R 202, Evonik, Essen, DE) was dissolved into acetone at 10 mg/mL concentration and used as an organic phase. A filtered Milli-Q® water, supplemented with 1% polyvinyl alcohol (PVA) (Mol wt: 30.000–70.000, Aldrich Chemical Co., Milan, IT), served as the aqueous phase. Rhodamine B (n°391, Radiant Dyes Laser, Wermelskirchen, DE) at 0.2 mg/mL concentration was supplemented into the organic phase to coprecipitate the tracer within PLA-based carriers. A laboratory-scale microfluidic system (NanoGenerator Flex M, Precigenome LLC San Jose, CAUSA), equipped with a passive staggered herringbone microchip, was employed to mix the organic and water phases[27,28]. The organic-to-aqueous phase ratio adopted was 1:1, while the total flow rate was 6

mL/min. Subsequently, the remaining surfactant was removed by washing the pellets following Optima™ XE-100 ultracentrifuge (Beckman Coulter, A94516), and particles were then collected through filtration.

The indirect analytical method was used to assess the encapsulation efficiency. For Rhod-B, the quantity of tracer not encapsulated in the supernatant was determined through UV/vis absorption spectroscopy (mod. Multiskan GO spectrophotometer, ThermoFisher Scientific) at the wavelength peak of 550 nm. A maximum concentration of Rhod-B at 0.2 mg/mL in the organic phase was selected, considering carriers' fluorescence intensity to be further detected by confocal microscopy and flow cytometry analysis. In this condition, a maximum encapsulation efficiency of 55% was achieved, as confirmed by the indirect analytical method using UV/vis absorption spectroscopy on the supernatant obtained post-centrifugation of the NP suspensions.

PLA-NPs characterization

NP morphology was determined through a Field Emission-Scanning Electron Microscope (FE-SEM mod. LEO 1525, Carl Zeiss SMT AG, Oberkochen, DE). Powder samples were placed on an aluminum stub with double-sided adhesive carbon tape. Subsequently, a thin coating of the gold film (250 A thickness) was applied to the sample using a sputter coater (mod.108 A; Agar Scientific, Stansted, UK) (Supplementary Figure S1).

To evaluate the stability of the PLA-NPs suspensions, NP size, distributions, and Zeta potential were determined using the dynamic light scattering (DLS) or the electrophoretic light scattering method (ELS) techniques with a Nano ZS Malvern Zeta Sizer (model 1000HSa, UK) at 25°C. The instrument was equipped with a He-Ne laser of 633 nm and a detector angle of 173°C.

To ensure accuracy, each measurement was repeated three times just after sample preparation, with a 60-second equilibration period between each measurement[28]. The software of the instrument was set to the automatic acquisition mode to facilitate the process (Supplementary Figure S2).

FITC-labelled polystyrene microplastics (PS-MPs)

Green, unmodified fluorescein (FITC)-labelled (λ, 468/508nm) polystyrene (PS) solid microspheres suspended in deionized water (1% solids suspension; 10 mL) of 1 µm diameter, 1.05 g/cm^3 density and a refractive index of 1.59 at 589 nm, were purchased from Thermo Fisher Scientific (USA).

PLA-NPs and PS-MPs suspension preparation

For in vivo treatments, PLA-NPs of 275 ± 75 nm (Rhodamine loading of 10 mg/g) and PS-MPs of 1 µm were diluted in embryo medium to the final tested concentrations of 0.1 and 1 mg/L. For cell treatments, stock suspensions of 1 mg/mL in cell culture medium of PLA-NPs and PS-MPs were prepared and then sonicated for 10 min at 10 °C, 37 kHz and 100 W 10 min before use. PLA-NPs and PS-MPs stock suspensions were subsequently further diluted in a cell culture medium to obtain the desired final concentrations of 10-50-100 and 300 µg/mL. The control was represented by the media without NPs and MPs. Suspensions were maintained in the dark and gently shaken before use.

Breeding zebrafish maintenance

The wild-type adult *Danio rerio* (6 months old) were raised at the Zebrafish facility of the Institute for Experimental, Comparative, Forensic and Aquatic Pathology "Slavko Bambir", Department of Chemical, Biological, Pharmaceutical, and Environmental Science, University of Messina. Adult zebrafish were kept in an automated Stand-Alone (Zebtec Multilinking System, Tecniplast, BUGUGGIATE (VA), Italy) under controlled conditions: photoperiod (light/dark cycle: 14:10 h), water quality (28 °C, pH 7.2, Conductivity 700 mS/cm, 6.00 ppm dissolved oxygen content (DO)). Fish were fed twice a day with both dry and live food (*Artemia salina*) at 3% of body weight (BW).

Zebrafish embryo/larvae exposure to PLA-NPs and PS-MPs

The embryos were obtained from breeding zebrafish groups consisting of mature adults paired in a 2 F:1 M ratio for successful reproduction. The day after breeding, zebrafish eggs were collected under a stereomicroscope (Leica M205C, Leica Microsystems Srl, Buccinasco (MI), Italy). PLA-NPs and PS-MPs suspensions were prepared using Embryo medium (E3; 15 mM NaCl, 0.5 mM KCl, 1 mM $CaCl_2$, 1 mM $MgSO_4$, 0.15 mM KH_2PO_4, 0.05 mM Na_2HPO_4, 0.7 mM $NaHCO_3$, at pH 7.3). The selected zebrafish embryos were exposed to suspensions of Rhodamine B-labelled PLA-NPs (red) or Fluorescein (FITC)-labelled PS-MPs (green) at 0.1 and 1 mg/L concentrations and incubated at 28 °C at a 14:10 h light: dark photoperiod regime up to 120 hpf. Experiments on zebrafish larvae were performed without ethical approval since, according to Directive 2010/63/EU, transposed into Italian law by D.lgs. 26/2014 on the protection of animals used for scientific research, zebrafish larvae up to five days (120 hpf) are not considered protected zebrafish forms and thus do not need ethical approval.

For all analyses performed at different time points (24, 72, 96 and 120 hpf), one-third of each suspension was refreshed daily. Fresh suspensions were sonicated each time to prevent the sedimentation and aggregation of PLA-NPs or PS-MPs and to ensure their homogenous distribution.

PLA-NPs and PS-MPs bioaccumulation analysis

The bioaccumulation analysis was performed on zebrafish embryos/larvae at different time points (24, 72, 96 and 120 hpf) to assess the uptake and localization of fluorescent PLA-NPs and PS-MPs within the developing zebrafish organism. Before observation, the zebrafish larvae of all groups (untreated and treated) were rinsed with distilled water to remove non-internalized or adhered PLA-NPs or PS-MPs and anesthetized with tricaine methanesulfonate (0.016% MS-222) solution to keep them stationary during observation. Fluorescent and brightfield images were captured under the fluorescent microscope in triplicate (Olympus BX-53, Japan). Three different larvae from each experimental group were considered for the analysis.

Zebrafish embryo toxicity (ZFET) assay and heart rate analysis

Zebrafish Embryo Acute Toxicity Test (ZFET) was performed on zebrafish embryos in accordance with OECD guidelines (OECD, 2013), Test n° 236, to investigate the acute toxic effects of PLA-NPs and PS-MPs at 0.1 and 1 mg/L. All ZFET validity criteria were met. The fertilized eggs were transferred into 96-well plates (1 embryo per well) with the test suspensions (PLA-NPs and PS-MPs at 0.1 and 1 mg/L), $n = 20$ eggs for each plate in triplicate of an experimental group, and the control groups were kept in only Embryo medium. Zebrafish embryos were incubated at 26 °C at a 14:10 h light: dark photoperiod regime. According to OECD guidelines, eggs of all experimental groups were monitored every 24 h to evaluate the apical lethal endpoints, i.e., coagulation, lack of somites, non-detachment of the tail, and absence of heartbeat.

Additionally, the heart rate was determined after 96 and 120 hpf as a physiological feature assessment. The heart rate was assessed through a video recording at the two timepoints on a representative number of larvae (biological triplicate) for each experimental group. The heart rate was analyzed as previously described by Capparucci et al.[29], .

Real-Time PCR for gene expression analysis

RNA was extracted from 18 zebrafish larvae for each experimental group at 72hpf and 120 hpf using the ReliaPrep™ Tissue Miniprep System (Cat.# Z6211, Promega). Briefly, a method for RNA purification from tissue samples has been used. Additional steps involving DNase treatment and ethanol precipitation are performed to ensure a purified, high-quality RNA yield by removing genomic DNA contamination and concentrating the RNA, respectively. The process concludes with the elution of RNA in Nuclease-Free Water. This method ensures efficient RNA isolation suitable for downstream applications. RNA was measured, and 1 µg of RNA at a 260/280 ratio > 1.8 was used for reverse transcription using a high-capacity cDNA kit (Applied Biosystem). Quantitative real-time PCR was performed in a step-one fast Real-Time PCR system (Applied Biosystems), using SYBR Green PCR MasterMix (Cat. no. 4309155, Life Technologies, Monza, Italy). PCR products were detected by the fluorescence of SYBR Green, a double-stranded DNA-binding dye. Primers were designed using BLAST® (Basic Local Alignment Search Tool, NCBI, NIH), and primer sequences are shown in Table 1. PowerUP™ SYBR™ Green Master Mix for qPCR (Applied Biosystem) was used for real-time RT-PCR experiments in a standard system under the following conditions: 50 °C for 2 min, 95 °C for 2 min, 95° for 15 s /60°C for 1 min (40 cycles). To ensure that only one product was amplified, all real-time RT-PCR experiments were followed with a melting curve analysis. For all experiments, gapdh RNA was used as the housekeeping gene for normalization. gapdh RNA levels were not affected by any treatment.

The relative mRNA expression level was calculated by the threshold cycle (Ct) value of each PCR product and normalized with gapdh using a comparative $2^{-\Delta\Delta Ct}$ method.

Histology

Five zebrafish larvae per group were prepared for histological examinations as previously described[30]. Briefly, entire zebrafish larvae at 120hpf were fixed in 4% paraformaldehyde (PFA) overnight at 4 °C, dehydrated by immersion in a graded series of alcohol, cleared in xylene and embedded in paraffin. Sections with a thickness of 5 µm obtained from paraffin blocks, were dewaxed in xylene for 10 min and, after being rehydrated by sequential immersion in decreasing ethanol concentrations and distilled water at RT, stained with hematoxylin and eosin (H&E) for histological analysis. The morphological evaluation was done by analyzing biological triplicate for each experimental group. The sections were examined by two expert pathologists, by using an optical microscope (Microscope Axioscope 5/7 KMAT, Carl Zeiss, Milan, Italy) connected to a digital camera (Microscopy Camera Axiocam 208 color, Carl Zeiss, Milan, Italy).

Cell culture, flow cytometry and Immunofluorescence analysis for uptake study

Human dermal fibroblasts (HDF, Gibco-Invitrogen cell culture, C0135C), were cultured in T25 tissue culture flasks with Dulbecco's modified Eagle's medium (DMEM, Sigma-Aldrich D6546) supplemented with 10% fetal bovine serum (FBS) (GIBCO Invitrogen, Milan, Italy), 100 U/ml penicillin and 100 U/ml streptomycin, and 2 mM L-glutamine and incubated at 37 °C, in a humidified atmosphere containing 5% CO_2.

Gene	Forward primer (5′ → 3′)	Reverse primer (5′ → 3′)	Accession number
hmox1a	TGGACAGAAACGCAGACCAC	GACTGCTCTTGCCAATCTCTCT	NM_001127516.1
sod2	CAAGGGACCACAGGTCTCATC	CTCGCTGACATTCTCCCAGT	NM_199976.1
sod1	GAACAAGGCCGTTTGTGTGC	ACTGGCTTCTTTTCACCCTCT	NM_131294.1
il1β	GTAACCTGTACCTGGCCTGC	AGACCCGCTGATCTCCTTGAG	NM_212844.2
il4	GCAGCATATACCGGGACTGG	ATGGCAGCATGCTTTGGTTT	NM_001170740.1
infγ1	TGGGCGATCAAGGAAAACGA	TTGATGCTTTAGCCTGCCGT	NM_212864.1
nos2a	AACTCTCTACAGCGGCGGAT	ATTCCTGGAAGTCCGATGCG	NM_001104937.1
tbx21	CGGGACAATTATGACACGCTG	AAGCGACTTTGAGGAAGGGG	NM_001170599.2
il13	CCCCAAAAGAGACAAAGGCAA	TCACACTTCAGGCCACTTCC	NM_001199905.1
tnfα	AGGAGAGTTGCCTTTACCGC	GTGAGTCTCAGCACACTTCCA	NM_212859.2
gapdh	ATACACGGAGCACCAGGTTG	AATACCAGCACCAGCGTCAA	NM_001115114.1

Table 1. Primer sequences used to assess gene expression.

Flow cytometry was used to evaluate the interaction between ~275 nm PLA-NPs, 1 µm PS-MPs and HDF. To perform cytometry analysis, HDF cells were seeded at 3×10^5 cells/mL in 6-multiwell plates and treated for 24 h 48 h, and 72 h at the following concentrations: 10 µg/mL, 50 µg/mL, 100 µg/mL, and 300 µg/mL with both rhodamine-labelled PLA-NPs and FITC-labelled PS-MPs. Untreated cells were used as a negative control. After each time point, cells were washed with PBS, detached by trypsinization, and resuspended in a 1 mL culture medium. Cells were then recovered by centrifugation (350 g, 5 min), the supernatant was discarded, and the cell pellet was resuspended in 0.3 mL PBS. Sample acquisition was performed by BD FACSuite software (BD Biosciences). Forward scattering area (FSC-A) and side scattering area (SSC-A) were used to separate living cells from debris and dead cells. All samples were run with the same PMT voltages, and a minimum of 10.000 events were recorded.

Immunofluorescence (IF) was used to evaluate the rhodamine-labelled PLA-NPs and fluorescein-labelled PS-MPs distribution within the HDF. For IF analysis, HDF cells were seeded at 3×10^4 cells/mL concentration in 8-well chamber slides and treated with Rhod-PLA-NPs- and FITC-PS-MPs- at 300 µg/mL concentration for 24 h. Then HDF cells were harvested and fixed in 2% paraformaldehyde (PFA, Sigma), washed with PBS 1X, and permeabilized with 0.1% Triton X-100 in PBS for 10 min. Subsequently, cells were incubated with Phalloidin-iFluor 488 (1:1000) (Abcam, ab176753, Cambridge, UK.) or Phalloidin-Tetramethylrhodamine B isothiocyanate (1:5000) (Merk, Darmstadt, Germany) for 30 min, washed with PBS 1X, and counterstained using 4',6-diamidino-2-phenylindole (DAPI, 1.5 µg/ml in distilled H_2O). All images were acquired at 40X magnification with identical settings of light, exposure time, and gain using a Leica laser-scanning confocal microscope (mod. TCS SP5; Leica Microsystems, Wetzlar DE). A quantitative analysis of the fluorescence intensity of Rhodamine and FITC, normalized to the total number of cells per field, was performed to confirm the cytometry analysis.

Statistical analysis

All statistical analyses were performed using the GraphPad PrismTM 4.0 program (GraphPad Software Inc., San Diego, CA, USA). Based on the analysis, where one (e.g., concentration) or more (e.g., concentration and time) independent variables were analyzed, one-way or two-way ANOVA, respectively, were used, followed by post hoc multiple comparison tests to ensure statistical rigor. In particular, the following statistics have been conducted in the single analysis: Ordinary one-way ANOVA with Tukey's multiple comparison test, was conducted for integrated fluorescence intensity assessment in the bioaccumulation assay; two-way ANOVA with Bonferroni's multiple comparison test was conducted for the evaluation of heartbeat rate and cytometry analysis; Ordinary one-way ANOVA with Holm-Sidak's multiple comparison test was conducted for gene expression evaluation. All data are presented as mean ± SD, and the level of statistical significance was set at $p < 0.05$.

Results

PLA-NPs and PS-MPs bioaccumulate in zebrafish larvae

The bioaccumulation of PLA-NPs (Fig. 1A) and PS-MPs (Fig. 1C) in zebrafish embryos or larvae has been assessed by exposing them to two concentrations (0.1 and 1 mg/L) of fluorescent ~275 nm Rhod B-labelled PLA-NPs (red) or 1 µm FITC-labelled PS-MPs (green) at 2–4 hpf and observed under fluorescent microscope at 24, 72, 96 and 120 hpf. The results demonstrated that both PLA-NPs and PS-MPs can accumulate in zebrafish larvae in a concentration-dependent manner. Before hatching (0–48 hpf), significantly higher fluorescence was observed around the embryonic chorion in both PLA-NPs and PS-MPs exposed embryos at 1 mg/L when compared to the controls (Fig. 1). With the aid of the light field images, we tried to estimate the localization of the PLA-NPs and PS-MPs: after hatching, the PLA-NPs and PS-MPs were found to adhere to the surface of larvae skin, especially at the highest concentration, while, at the protruding mouth stage (72 hpf), the yolk sac and digestive tract seemed to be the main accumulation sites for both PLA-NPs and PS-MPs. In zebrafish's early larval stage (96-120hpf), the accumulation and internalization of PLA-NPs and PS-MPs appeared to happen in the gastrointestinal (GI) tract at both concentrations. At 120 hpf, PLA-NPs seem to be accumulated especially in the proximal part of GI tract corresponding to the anterior intestinal bulb, where PLA-NPs formed aggregates resulting in a bulky mass which seem to have difficulty in progressing along the alimentary canal (Supplementary Figure S3). To evaluate the fluorescence intensity trend during bioaccumulation, we analyzed the fluorescence intensity of Rhod B/PLA-NPs and FITC-labelled PS-MPs, respectively. While the fluorescence intensity of PLA-NPs appears to increase in a time- and dose-dependent manner up to 120 hpf, PS-MPs appear to decline at 120 hpf. Overall, these results demonstrated absorption and similar concentration-dependent biodistribution of both PLA-NPs and PS-MPs in zebrafish at early life stages.

ZFET analysis and physiological effects: PLA-NPs and PS-MPs induce contrasting alterations in heartbeat rate

In the present study, none of the experimental groups (PLA-NPs and PS-MPs), at both low (0.1 mg/L) and high (1 mg/L) concentrations tested, showed visible developmental alterations or mortality in zebrafish embryos/larvae compared to the untreated control group. Moreover, hatching of zebrafish larvae occurred between 48 and 72 hpf, as in control groups, and none of the embryos/larvae exhibited evident developmental defects up to 120 hpf (Fig. 2A).

Regarding physiological assessment, heartbeat rate was measured at 96 hpf and 120 hpf in both experimental groups and for both concentrations (Fig. 2B, C). In the PLA-NPs exposed group, a significant decrease in heartbeat rate was observed at the highest concentration compared to the control (Fig. 2B).

Contrarily, in the PS-MPs exposed experimental group, a significant increase in heartbeat rate was observed at both concentrations compared to the control group (CTRL) (Fig. 2C). Overall, the data demonstrated that PLA-NPs appear to promote heartbeat rate deceleration, while PS-MPs seem to promote heartbeat rate acceleration,

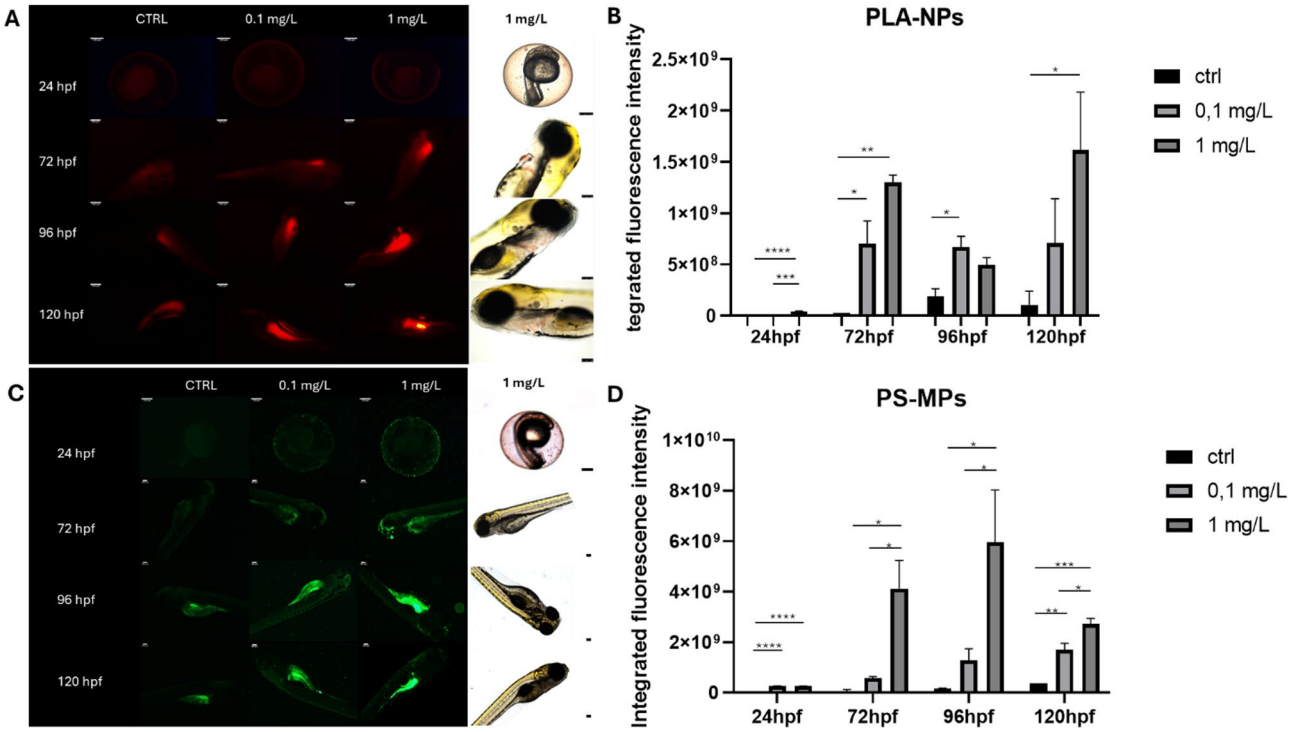

Fig. 1. Fluorescence intensity of larvae exposed to Rhod B-labelled PLA-NPs and FITC-labelled PS-MPs. **(A)** Representative images of control (CTRL) and 250 nm Rhod B-labelled PLA-NPs exposed embryos or larvae at 24, 72, 96 and 120hpf, at low (0.1 mg/L) and high (1 mg/L) concentrations; Bright-field images of 1 mg/L were added to show larvae orientation. Magnification 10X, scale bar 250 µm (24 hpf embryos) and 100 µm (72-96-120 hpf larvae). **(B)** Bar graph reports integrated fluorescence intensity (area x fluorescence intensity) ± SD at 24, 72, 96 and 120hpf larvae exposed to low and high concentrations of Rhod B/PLA-NPs; **(C)** Representative images of control (CTRL) and 1 µm FITC-labelled PS-MPs (green) exposed embryos or larvae at 24, 72, 96 and 120hpf, at low (0.1 mg/L) and high (1 mg/L) concentrations. Bright-field images of 1 mg/L were added to show larvae orientation. Magnification 10X, scale bar 250 µm (24 hpf embryos) and magnification 5X, scale bar 100 µm (72-96-120 hpf larvae). **(D)** Bar graph reports integrated fluorescence intensity (area x fluorescence intensity) ± SD at 24, 72, 96 and 120hpf larvae exposed to low and high concentrations of FITC/PS-MPs. Integrated fluorescence intensity was analyzed using data from biological triplicate for each experimental group. Statistical analysis by Ordinary one-way ANOVA followed by Tukey's multiple comparison test, was conducted. The p-values < 0.05 were considered statistically significant: (*$p < 0.1$; **$p < 0.01$; ***$p < 0.001$; ****$p < 0.0001$); p-values > 0.05 were considered not significant (not shown).

suggesting a possible indirect effect on heart of larvae treated with PLA-NPs or PS-MPs even though in an opposite way (Supplementary Figure S4).

PLA-NPs affect the antioxidant defense system, activate immune responses, and cause inflammation, likewise PS-MPs

Oxidative stress- and inflammation-related genes were evaluated in zebrafish larvae exposed to low (0.1 mg/L) and high (1 mg/L) concentrations of PLA-NPs or PS-MPs, at early (72 hpf) and late (120 hpf) developmental stages. In the PLA-NPs exposed group, the oxidative stress markers (*hmox1a*, *sod1*, *sod2*, *nos2*) were all significantly upregulated at both developmental stages (Fig. 3A-D), suggesting acute oxidative stress induction potential. Moreover, PLA-NPs either caused or induced upregulation of all studied pro-inflammatory cytokines (*il1β*, *tnfα*, *infγ*, and *il13*) at 120 hpf and at the highest concentration (Fig. 3E, F,H, I), suggesting inflammation. However, the trend of *il1β* and *infγ*, which seem to be downregulated at 72hpf and upregulated at 120 hpf (Fig. 3E and I), might be a way for the zebrafish system to initially dampen the inflammatory response.

Similarly, the PS-MPs exposure resulted in dysregulation of antioxidant activity, suggested by a drastic initial (72hpf) upregulation and later (120 hpf) downregulation of both heme oxygenase-1a (*hmox1a*) (Fig. 4A) and nitric oxide synthase 2 (*nos2*) (Fig. 4B). Opposite results were seen in the expression levels of superoxide dismutase 1 (*sod1*) and manganese-superoxide dismutase (*sod2*), with significant downregulation of *sod1* (Fig. 4C) and significant upregulation of *sod2* (Fig. 4D) at 120 hpf. The exposure to PS-MPs also determined a significant upregulation of pro-inflammatory markers. Interleukin 1 beta *(il1β)* was induced at 120 hpf at the highest concentration (Fig. 4Eb), while tumor necrosis factor alfa (*tnfα)* and interferon-gamma *(infγ*) were upregulated at 72 hpf, at low (Fig. 4Fa) and high (Fig. 4Ia) concentrations, respectively. The anti-inflammatory cytokine *il4* was found to be induced at 72 hpf, but not at 120 hpf in both groups (Figs. 1G and 2G), suggesting an early immunity regulation. Remarkably, a significant upregulation of T-box transcription factor 21 (*tbx21*)

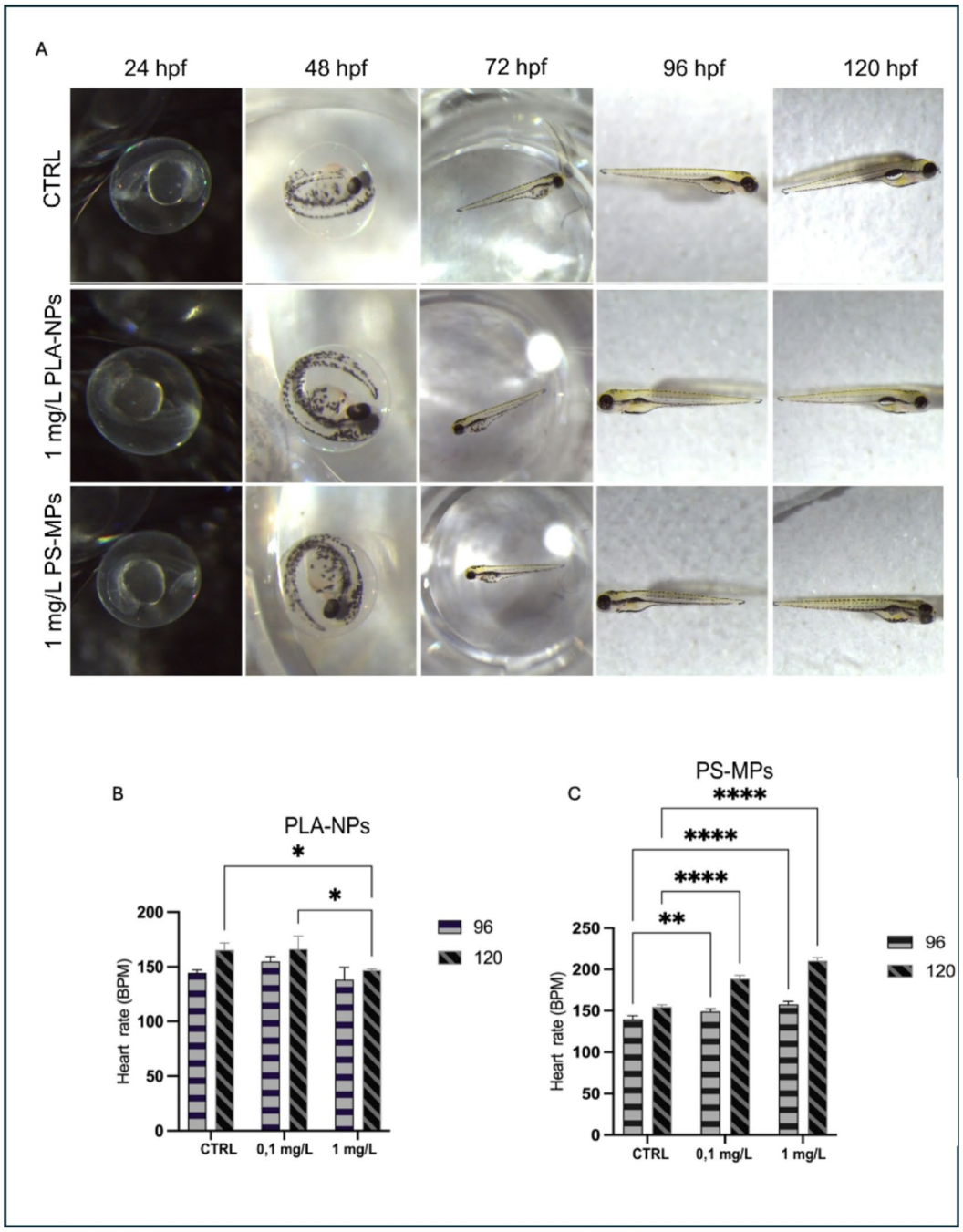

Fig. 2. ZFET and heartbeat rate analysis. **(A)** ZFET and representative images of the control group and experimental groups at the highest concentration (1 mg/L), captured under a stereomicroscope for morphologic developmental evaluation of zebrafish embryos/larvae at 24, 48, 72, 96 and 120 hpf. **(B)** Heart rate statistical analysis of zebrafish larvae exposed to low (0.1 mg/L) and high (1 mg/L) PLA-NPs at 96 and 120 hpf. **(C)** Heart rate statistics of zebrafish larvae exposed to low (0.1 mg/L) and high (1 mg/L) PS-MPs at 96 and 120 hpf. Heart rate was analyzed using data from biological triplicate for each experimental group. Statistical analysis by two-way ANOVA with Bonferroni's test for multiple comparisons was conducted. (*$p < 0.05$; **$p < 0.01$; ****$p < 0.0001$).

activity was observed in both groups at 72 and 120 hpf (Figs. 1J and 2J) suggesting the activation of type 1 immune response.

PLA-NPs did not induce vacuolization in brain and liver tissues, as for PS-MPs-treated larvae

Sections of hematoxylin and eosin-stained zebrafish larvae at 120 hpf exposed to PLA-NPs showed no evident alterations in brain and liver compared to the controls (Fig. 5B, C). On the contrary, the PS-MPs-exposed group

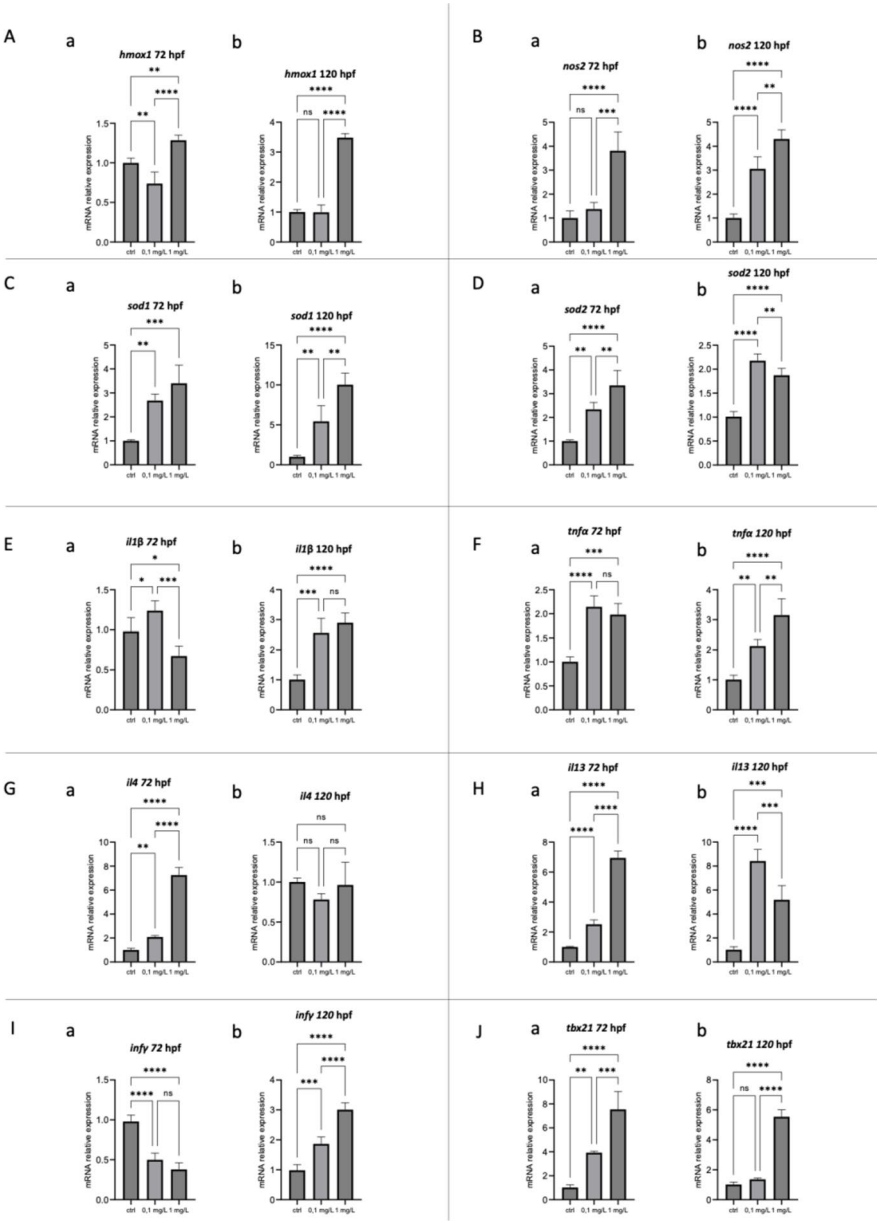

Fig. 3. Real-time PCR for gene expression analysis in PLA-NPs exposed larvae at 72 and 120 hpf. **(A-J)** Bar graphs reporting the relative mRNA expression levels ± SD for **(A)***hmox1*; **(B)***nos2*; **(C)***sod1*; **(D)***sod2*; **(E)***il1β*; **(F)***tnfα*; **(G)***il4*; **(H)***il13*; **(I)***infγ*; **(J)***tbx21*, measured respectively at **(a)** 72 hpf and **(b)** 120 hpf. Gene expression was analyzed using data from biological triplicate. Six larvae were used for each replicate. Statistical analysis by Ordinary one-way ANOVA with Holm-Sidak's test for multiple comparisons was conducted. The p-values < 0.05 were considered statistically significant: (*$p < 0.1$; **$p < 0.01$; ***$p < 0.001$; ****$p < 0.0001$); p-values > 0.05 were considered not significant (ns).

showed morphological alterations at all examined tissue levels (Fig. 5D, E) compared to the controls (Fig. 5A). Larvae exposed to both low and high concentrations of PS-MPs demonstrated the presence of spherical empty spaces creating a tissue discontinuity (Fig. 5D, E) in both liver and brain.

PLA-NPs and PS-MPs internalize in a concentration-dependent manner in HDF cells

Flow cytometry analysis was carried out to evaluate the potential of PLA-NPs and PS-MPs to be internalized by HDF cells (Figs. 6 and 7). Cells were treated separately with PLA-NPs and PS-MPs at the final concentrations of 10, 50, 100, and 300 µg/mL for 24, 48 and 72 h. Results show an increased uptake of PLA-NPs in a concentration-dependent manner (Fig. 6a, b). However, only 6% of cells were positive in the presence of ~ 275 nm PLA-NPs, at the highest concentration of 300 µg/mL, already after 24 h, and this trend was maintained up to 72 h. In contrast, the 1-µm PS-MPs internalize within the cells in both time- and concentration-dependent manner (Fig. 7). The percentage (around 33%) of PS-MPs positive cells was observed at the highest concentration of 300 µg/mL at

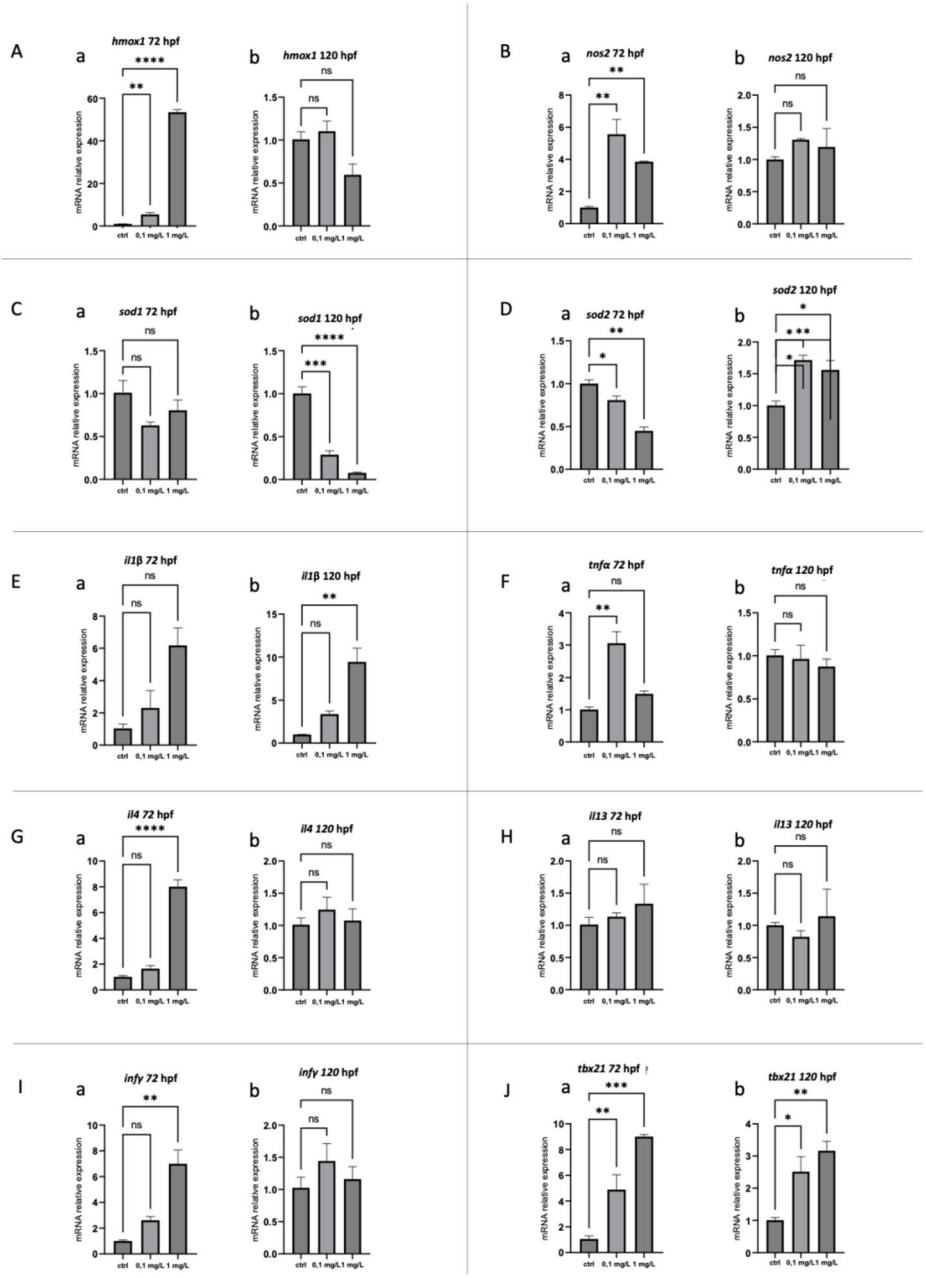

Fig. 4. Real-time PCR for gene expression analysis in PS-MPs exposed larvae at 72 and 120 hpf. **(A-J)** Bar graphs report the relative mRNA expression levels ± SD for **(A)***hmox1*; **(B)***nos2*; **(C)***sod1*; **(D)***sod2*; **(E)***il1β*; **(F)***tnfα*; **(G)***il4*; **(H)***il13*; **(I)***infy*; **(J)***tbx21*, measured respectively at **(a)** 72 hpf and **(b)** 120 hpf. Gene expression was analyzed using data from biological triplicate. Six larvae were used for each replicate. Statistical analysis by Ordinary one-way ANOVA with Holm-Sidak's test for multiple comparisons was conducted. The p-values < 0.05 were considered statistically significant: (*$p < 0.1$; **$p < 0.01$; ***$p < 0.001$; ****$p < 0.0001$); p-values > 0.05 were considered not significant (ns).

24 h, this trend further increased, reaching 45% of cells internalizing PS-MPs at 72 h (Fig. 7a, b). These results indicated that HDF cells can uptake PLA-NPs of ~275 nm, even though PS-MPs of 1 µm exhibited a better performance in cell uptake despite the presence of a higher diameter. A quantitative analysis of fluorescence intensity of Rhodamine and FITC, confirmed the data of flow cytometry and the HDF uptake potential of both PLA-NPs and PS-MPs at the highest concentration (Supplementary Figure S5). Moreover, IF analysis of plastic distribution inside the cells showed that PLA-NPs accumulate in the HDF cytoplasmic region, with a tendency to concentrate in perinuclear space (Fig. 6c), likewise PS-MPs (Fig. 7c).

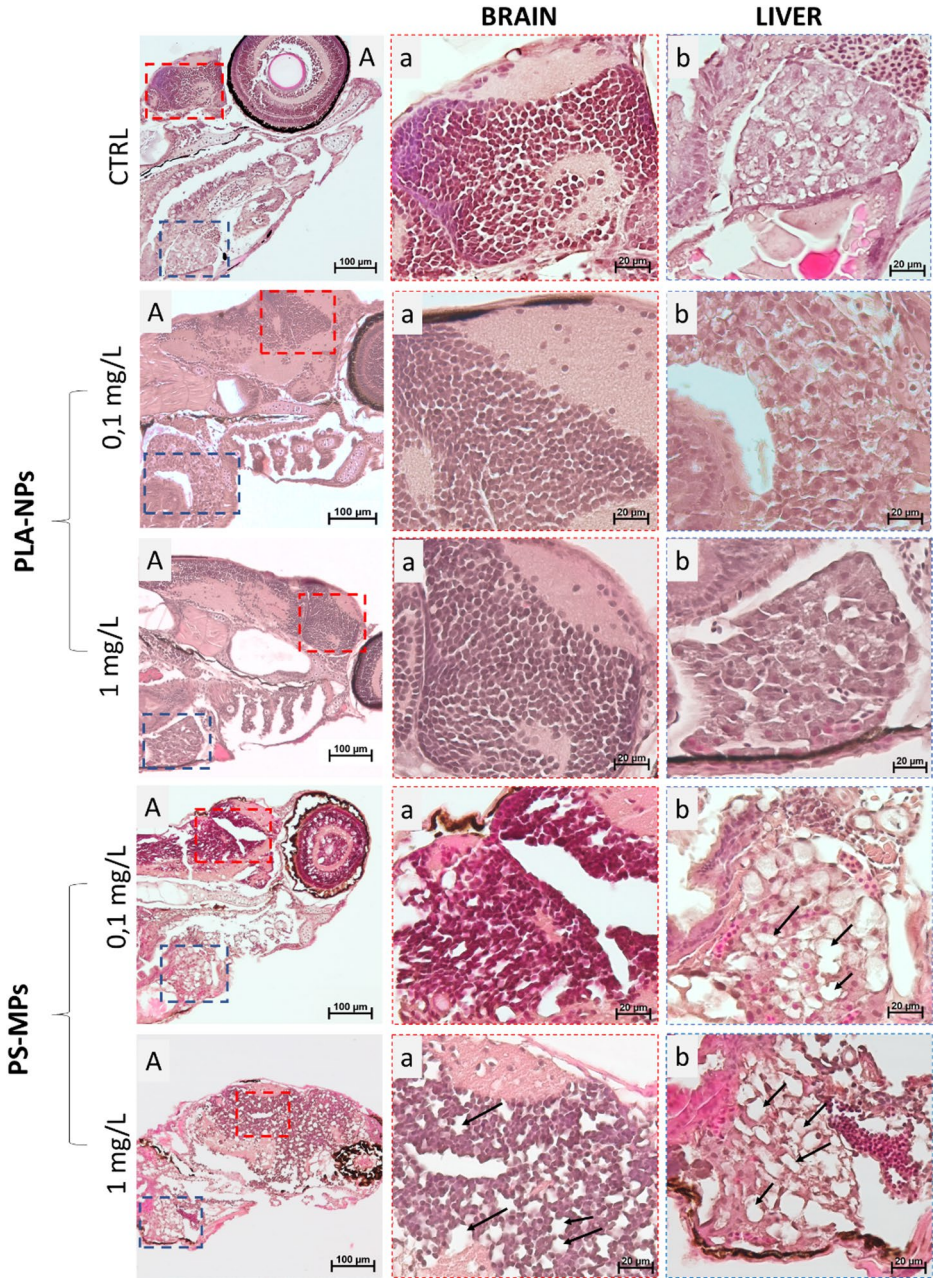

Fig. 5. Morphological features of zebrafish larvae at 120 hpf exposed to low (0.1 mg/L) and high (1 mg/L) concentrations of PLA-NPs and PS-MPs. Three larvae of 120 hpf for each experimental group were used for morphological assessment. **A-E)** Representative images of H&E staining **(A)** control; **(B)** PLA-NPs 0.1 mg/L; **(C)** PLA-NPs 1 mg/L; **(D)** PS-MPs 0.1 mg/L; **(E)** PS-MPs 1 mg/L. Magnification 10X and 40X, scale bar 20 and 100 µm. **a-b)** Representative detailed images of H&E staining: **(a)** brain and **(b)** liver of the related groups **(A-E)**. The vacuolization is indicated by black arrows. Magnification 40X, scale bar 20 µm.

Discussion

The main aim of the present study was to evaluate the effects of bio-based PLA-NPs exposure on zebrafish (*Danio rerio*) embryos/larvae, using the well-known PS-MPs as a positive control of damage induction related to microplastic pollution, in the model. The freshwater zebrafish model was chosen for the present study due to its genetic similarity with the human genome and its common use for several research purposes[31–33], which proves itself to be an highly versatile and informative model organisms in both toxicology and ecotoxicology, and it is increasingly accepted as alternative models to traditional animal testing, despite being a vertebrate model. Indeed, the biological effects caused by harmful agents on this model, have often been a starting point for understanding their impact on the human organism.

Our results suggest that the primary site of accumulation of PLA-NPs and PS-MPs is presumably represented by the GI tract, especially at the latest stages of development, in accordance with other studies[34]. Nonetheless,

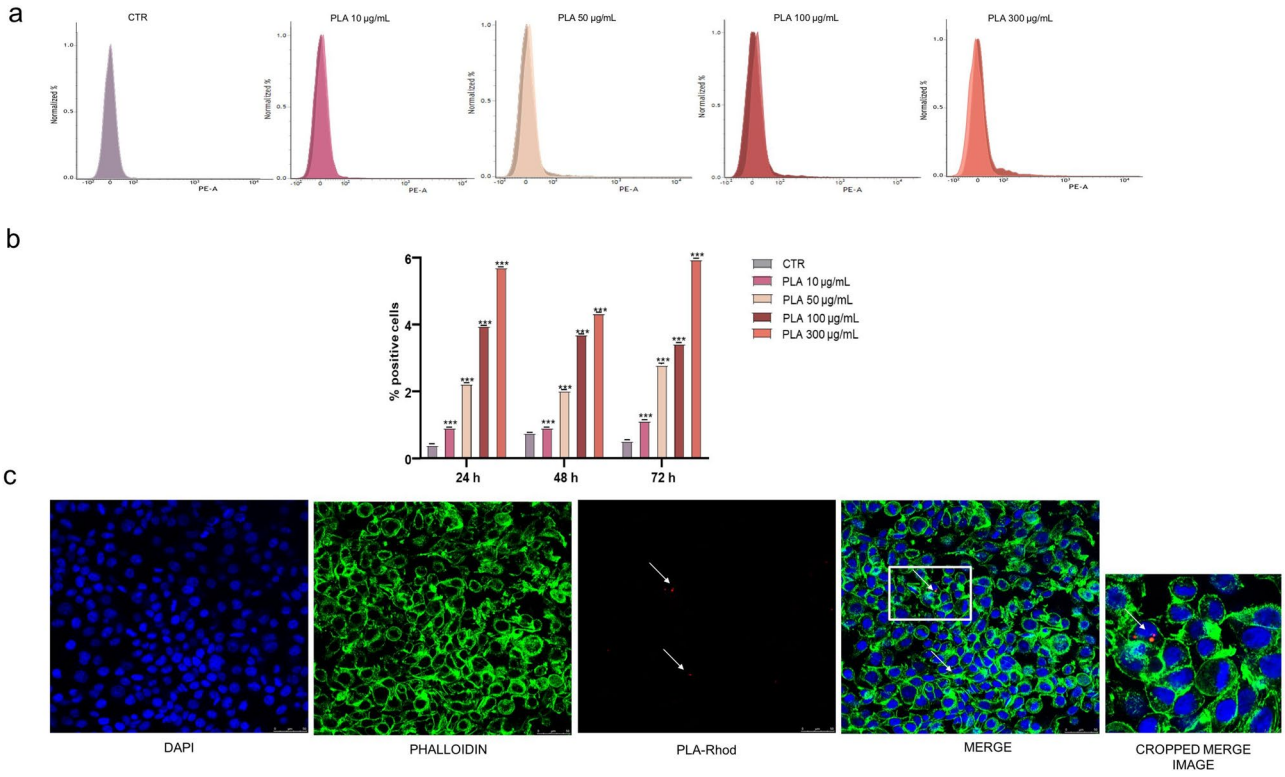

Fig. 6. Rhodamine-labelled PLA-NPs internalization through flow cytometry and confocal microscopy. Rhodamine-labelled PLA-NPs internalization analysis was assessed by flow cytometry (a, b) and confocal microscopy (c). For flow cytometry 3×10^5 cells/mL were treated for 24, 48 and 72 h at the concentrations of 10, 50, 100 and 300 µg/mL of rhodamine-labelled PLA-NPs. Panel (a) reports a representative FACS histogram of HDF internalization of Rhodamine-labelled PLA-NPs. Bar graph in panel (b) reports the % ± SD of fluorescent positive cells for each concentration and time point tested. Statistical analysis was performed using two-way ANOVA ($*p < 0.05$, $**p < 0.01$, $***p < 0.001$), followed by Bonferroni's post hoc test. All the experiments were performed in triplicate. (c) Confocal representative images of Rhodamine-labelled PLA-NPs uptake in HDF. Nuclei were stained with DAPI (blue), the cytoskeletons were stained with Phalloidin (green), and Rhodamine-labelled PLA-NPs were represented by red fluorescence (white arrows). Magnification 40X, scale bar 50 µm.

we noticed a different accumulation arrangement in these two experimental groups. In the PLA-NPs exposed larvae of 72hpf, we observed a neglectable skin adhesion of PLA-NPs, while their accumulation may be detected at the GI level, especially at the highest concentration (Fig. 1A). On the contrary, in the PS-MPs treated group, the adhesion of PS-MPs on the surface of the larva skin could be noticeable at the highest concentration. The adhesion may be due to the presence of mucous cells in the outermost layer of zebrafish skin[35]. The secretion of mucus on the skin surface represents an essential fish defense against environmental stress factors, and even small differences at this level may lead to injury and inflammation[36]. This diverse adhesion and absorption behavior of PLA-NPs and PS-MPs might be due to the different stress levels induced by plastics, which may result in dissimilar production of mucus and can be the result of diverse chemical properties and smaller size of PLA-NPs (~ 275 nm) compared to PS-MPs (1 µm). Moreover, the protruding-mouth stage of the larvae occurring between 72 and 96 hpf[37], probably enables the early entrance of the nanoparticles through the ingestion route. We conjecture that in zebrafish larvae of 96–120 hpf, corresponding to the early larva stage[37], characterized by food-seeking behavior, the accumulation and internalization of both PLA-NPs and PS-MPs might mainly occur in the GI tract. Although in-depth tissue-specific localization analyses are necessary, as well as experiments beyond 120 hpf, this hypothesis is supported by the decrease in bioaccumulation that we observed in larvae at 120hpf treated with PS-MPs, which on the contrary we did not observe in larvae treated with PLA-NPs, at the same time point, at a concentration of 1 mg/L (Fig. 1B and D). This, together with what is shown in the supplied video (Supplementary Figure S3), i.e., what appears to be a blockage of the PLA-NPs passage from the intestinal tract of the larva, suggests that PLA-NPs have greater aggregating capacities than PS-MPs. It may be due to the PLA-NPs characteristics in terms of nanometer size, physico-chemical, and surface properties[38,39]. PS-MPs can probably be more easily eliminated from the gastrointestinal tract of the larvae, determining a decrease in bioaccumulation rate, contrary to what happens for larvae treated with PLA-NPs, where the aggregates limit the excretion of nanoparticles, sustaining the high bioaccumulation rate detection. Anyway, this hypothesis needs further investigation. Overall, the results demonstrated that both particles are absorbed by the zebrafish system in a concentration-dependent manner (Fig. 1).

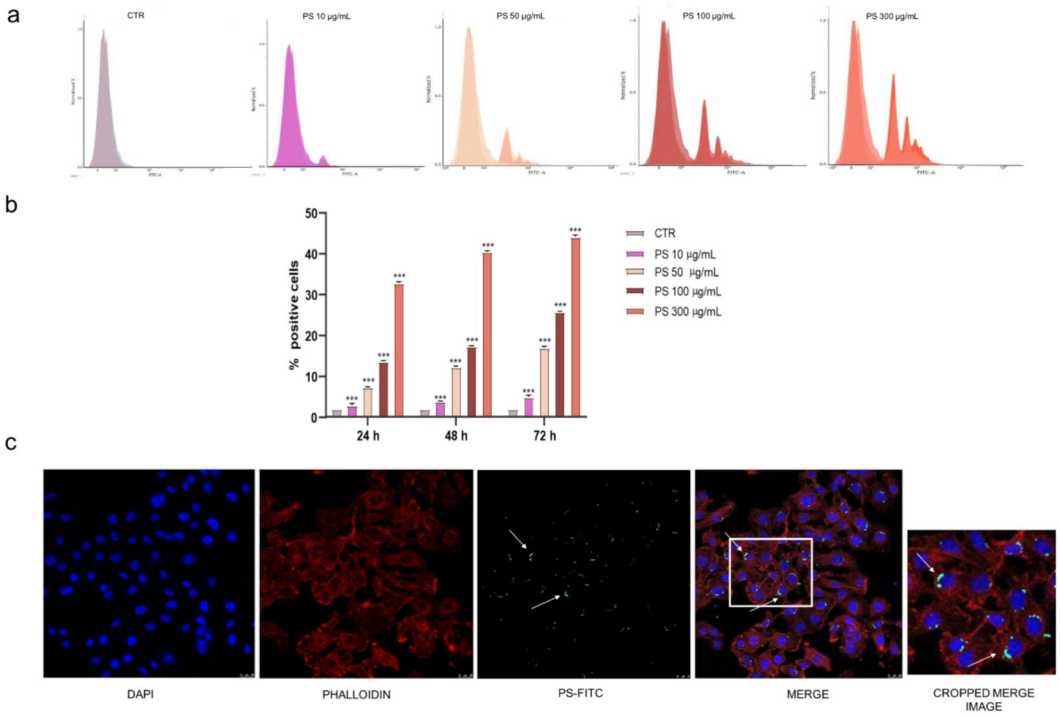

Fig. 7. FITC-labelled PS-MPs internalization through flow cytometry and confocal microscopy. FITC-labelled PS-MPs internalization analysis was assessed by flow cytometry (**a, b**) and confocal microscopy (**c**). For flow cytometry 3×10^5 cells/mL were treated for 24, 48 and 72 h at the concentrations of 10, 50, 100 and 300 µg/mL of FITC-labelled PS-MPs. Panel (**a**) reports a representative FACS histogram of HDF internalization of FITC-labelled PS-MPs. Bar graph in panel (**b**) reports the % ± SD of fluorescent positive cells for each concentration and time point tested. Statistical analysis was performed using two-way ANOVA ($*p < 0.05$, $**p < 0.01$, $***p < 0.001$), followed by Bonferroni's post hoc test. All the experiments were performed in triplicate. (**c**) Confocal representative images of FITC-labelled PS-MPs uptake in HDF cells. Nuclei were stained with DAPI (blue), the cytoskeletons were stained with Phalloidin (red), and FITC-labelled PS-MPs were represented by green fluorescence (white arrows). Magnification 40X, scale bar 50 µm.

In vivo evaluation demonstrated that at the used concentrations, none of the treatments caused mortality, changes in hatching rate, body length, or visible developmental malformations; however, alterations in heartbeat rate were observed in the PLA-NPs exposed group at 96 and 120 hpf with the induction of bradycardia, especially at the highest concentration (Fig. 2C). The bradycardia has been associated with the accumulation of lactic acid within the fetal human myocardium and the consequent reduced force of contraction and cardiac output[40]. It is a plausible scenario that the accumulation of lactic acid within the zebrafish larvae bodies might occur due to the biodegradation and breaking down of PLA-NPs; as a matter of fact, during PLA degradation the buildup of lactic acid, which was observed also during biodegradation of medical implant in human[41], can result in a lower pH, which might trigger inflammation and irritation in the tissues[42]. Lactic acid may interfere with endogenous metabolites, inducing metabolic alterations and leading to the lactic acidosis with its negative consequences on the organs and behaviour as proposed by other studies[13,19,43,44]. However, the mechanism underlying the bradycardia induction in the present study needs further investigation. In addition, in the PLA-NPs-treated group, two individuals exposed to the highest concentration of PLA-NPs showed temporary cardiac arrest, followed by the beating activity after some seconds (see Supplementary Figure S4), suggesting an electrical issue or myocardial depression. However, it was a random detection and studies on grater individual numbers should be conducted at the indicated concentration to better investigate this phenomenon. Opposing results were observed for the heartbeat rate after exposure to PS-MPs. Indeed, the larvae of 96 and 120 hpf exposed to PS-MPs demonstrated a significant heartbeat acceleration (Fig. 2B), as detected in the study by La Pietra et al.[25], suggesting a possible heart function alteration. In this regard, it is important to underline that all the larvae from both treated and untreated groups have been exposed to MS-222 (0.016%) to avoid their movements during videoing, as previously described[45,46]. Regarding the use of MS-222 (0.016%) for a short-term period in larvae, its reliability is unclear in terms of heartbeat measurements, and contrasting results are reported in the literature[47,48]; therefore, this limitation should be considered. Furthermore, literature is lacking in knowledge about the toxic effect of PLA-NPs on heart and how these nanoparticles may reach the cardiac tissue, nevertheless, it is plausible that the PLA-NPs may behave like the PS-MPs, reported to reach several tissues, such as myocardium, through their gut uptake, due to impaired intestinal barrier integrity and blood distribution in zebrafish[49,50]. Moreover, an elevated concentration of MPs in feces of patients affected by vascular calcification and a strong relationship between vascular calcification score and the quantity of MPs, have been

detected in humans[50]. Additional research is necessary to better understand the link between plastic exposure and cardiovascular effects.

It is widely recognized that exposure to exogenous agents such as environmental toxicants, pathogens, ultraviolet light, and various chemical compounds induces molecular alterations of cellular homeostasis[51]. The most studied markers of cellular stress, representing a sensitive indicator of acute stress induction, are represented by oxidative stress and inflammation ones.

Since the organism's antioxidant ability is one of the most important defense systems, as it is directly responsible for the maintenance of the redox balance, acting against ROS overproduction and thus alleviating oxidative stress[52], in the present study the antioxidant enzyme (*hmox1*, *sod1*, *sod2*, *nos2*) expression levels in developing zebrafish exposed to PLA-NPs and PS-MPs, was investigated. The overall results (Figs. 3 and 4) showed the induction of oxidative stress in both PLA-NPs and PS-MPs exposed groups, but it occurred with different adaptation responses or hormesis[53]. PLA-NPs exposure determined a significant increase in the expression of all investigated antioxidant markers (Fig. 3), suggesting that the PLA-NPs exert pro-oxidant effects and lead to acute and probably reversible, oxidative stress induction[54].

On the contrary, after the PS-MPs treatment, the antioxidant enzymes such as *hmox1*, *sod1* and *nos2* decreased in exposed zebrafish larvae at 120 hpf, after their earlier (72hpf) increase (only *hmox1* and *nos2* statistically significantly) (Fig. 4), suggesting re-modulation and disruption in the antioxidant defense system of the larvae after longer exposure time[55], and the redox imbalance in favor of free radicals and reactive oxidants with chronic oxidative stress onset[53]. The latter occurred, therefore, in a time exposure-dependent manner, confirming the results of numerous other studies[8,56–58].

Similarly, also the expression of inflammatory markers (*il4*, *il13*, *il1β*, *tnfα*, *infγ*, *tbx21*) appeared different in the two experimental groups. In PLA-NPs exposed groups, a significant induction of pro-inflammatory markers (*il1β*, *tnfα*, *infγ*, *tbx21*) was detected, especially at the latest stages and at the highest concentration (Fig. 3), suggesting acute inflammation occurrence, probably sustained by the strong activation of the antioxidant system and acute oxidative stress induction[59]. Moreover, the increase in anti-inflammatory cytokines *il4* and *il13* was observed at the early stage (72 hpf), followed by their downregulation at the latest stage (120hpf), confirming the PLA-NPs-induced immunotoxicity. However, these results need to be better investigated since during the early stages of development, zebrafish larvae depend solely on innate immune responses[60] and a more comprehensive effect of PLA-NPs on the immune system is necessary to be assessed after 4 weeks of development.

A contrary response in the expression of inflammatory markers was seen in the PS-MPs exposed group, where a significant induction of *il4*, *infγ*, *tnfα* and *tbx21* was observed at the early developmental stage (72 hpf), while it decreased at the latest one (120hpf), where significant induction of only *il1β* was detected at the highest concentration (Fig. 4). These results suggest a total dysregulation of the immune response, which probably occurs due to the chronic loss of redox balance[61]. Since molecular alterations were observed, the morphological features in zebrafish larvae tissues at both experimental concentrations were investigated (Fig. 5). In the present study, we did not detect the vacuolisation process in brain and liver tissue of PLA-NPs treated larvae; instead, this process was detected in PS-MPs treated zebrafish larvae, at the used concentrations, confirming data from the literature. These organs, in addition to appearing severely damaged by polystyrene-based plastics in the zebrafish model[62–65], have been recently found to be worryingly contaminated in humans[66,67]. The PS-MPs associated with other molecules have been detected to cause vacuolisation of zebrafish gonads[68,69]. Furthermore, the hepatic vacuolisation process is reported to be associated with activation of ROS signalling and the co-treatment of both PS-MPs and sulfamethoxazole in zebrafish[63], and with orally administered 0.2 mg of PLA-MNPs in mice[70], suggesting the morphological alteration potential of polylactic acid microplastics at higher concentrations. Cytoplasmic matrix and mitochondrial vacuolisation have also been detected in goblet cells of intestinal villi of PS-NPs treated zebrafish[71]. In this regard, *il1β*, which normally has the role to maintain the intestinal barrier, was found upregulated at 120 hpf, both in PLA-NPs and PS-MPs treated zebrafish. These data confirm what is reported in the literature[71] and suggest a strong stress response at the GI tract level, which may be related to an inflammatory reaction, characterized by accumulation of immune cells and fluid in the affected tissues. This may contribute to the vacuolization process. However, the latter has not been detected herein the PLA-NPs treated group; further in-depth experiments (e.g., chronic, longer-term exposure) are needed to assess whether the vacuolization process can also be caused by polylactic acid nanoplastics. Moreover, decrease in mitochondrial function related to oxidative stress in the intestinal tract of zebrafish after PS-MPs exposure has been also associated with the increase of SOD activity[72]. Curiously, the opposite expression profile was detected for *sod2* as it appeared significantly decreased at 72 hpf and significantly increased at 120hpf in PS-MPs treated larvae, suggesting a late activation of the mitochondrial antioxidant system. While both *sod1* and *sod2* are significantly increased in PLA-NPs exposed larvae.

Despite the clear cellular stress profile detected at gene expression level, it appears unclear why the morphological alterations at the examined tissue level of PLA-NPs treated zebrafish have not been detected here. Since the previous study on mice demonstrated the morphological alteration induction after exposure to airborne PLA-M/NPs at higher concentrations[70], it may be that the concentrations used in the present study were too low to induce tissue structural changes. Moreover, it may also depend on the fact that NPs at low concentration may mainly induce nuclear damage since the particles can cross the nuclear membrane and induce DNA damage, not detectable at tissue levels at this point of experiments. Further studies are necessary to clarify this aspect.

Our results in zebrafish underline the capability of PLA-NPs to reach tissues, causing cellular stress similar to the PS-MPs-related one. To shed light on the capability of PLA-NPs to be potentially toxic in humans, we studied the internalization of PLA-NPs and PS-MPs in human HDF to mimic the human biological skin barrier[73]. Thus, the cell uptake of MPs/NPs has been assessed through flow cytometry and IF analysis. The results showed HDF uptake potential for both PLA-NPs and PS-MPs, raising new questions about the safety of PLA-based products for human health. PLA-NPs demonstrated a lower internalization rate (Fig. 6) when compared to PS-MPs, (Fig.

7). However, it is conceivable that it was due to the aggregation of the NPs before reaching the cell membrane, reducing the availability of NPs to be internalized within the cells. Accordingly, our group demonstrated that reducing the size of PLA-NPs leads to almost 100% internalization in other cell types[28]. Nevertheless, as for the zebrafish model, the results showed that the PS and PLA particles under consideration in this study may also be absorbed by a human cell type.

Another explanation regards the chemical properties of the polymers PLA versus PS, which possess different surface charges and physicochemical properties, which probably influence the interaction and their transport through the cell membrane[74]. Therefore, the aggregation capabilities of plastics, in vitro and *vivo*, in a medium, or within an organism (as seen in the GI of zebrafish larvae), may be different and could be size-dependent, physicochemical property-dependent, or environment-dependent. We do not exclude that smaller PLA-NPs may penetrate the cell membrane more efficiently, both in vitro and in vivo. Our laboratory plans to further investigate the effects of the smaller-sized PLA-NPs on developing zebrafish and their uptake potential in HDF.

Moreover, since the plastic pollution represents a severe global crisis with most of it accumulating in the seas and oceans, it is worth noting here that salt in water, as the weight of the water column, differences in temperatures and pH in marine ecosystem may diversify the bioaccumulation processes of plastic derivatives in human and fish tissues. For this reason, it would be worthwhile investigating the effects of the PLA-derived degradation products under the marine water conditions, to further confirm the results of the present study.

Conclusions

Until recently, the presence of the 'invisible' plastic pollution has been considered harmless; however, today it is recognized that the petroleum-based derived MPs and NPs constitute a great concern for all living organisms, and methodologies capable of eliminating these small particles from the aquatic and terrestrial environment are still lacking. Alternative biodegradable bioplastics have been introduced to reduce the invisible plastic pollution, however, increasing evidence suggest that these latter need controlled conditions to fully degrade, which are not present in natural ecosystems. Indeed, it appears fundamental to further investigate the effects of the degradation products of the bio-based macro- and microplastics, which give rise to heterogeneous-sized NPs, and which, in turn, may have varied behaviour and consequently evoke biological effects in terms of bioaccumulation and physiopathology in different species. For this reason, the present study investigated the effects of environmentally relevant in size and concentration PLA-NPs in developing zebrafish and compared the results with the well-known harmful effects of PS-MPs exposure to validate the reliability of the experiment. In conclusion, our findings suggest that, proportionally to the fossil-based PS-MPs, PLA-NPs bioaccumulate within the developing zebrafish organs, determining heartbeat rate changes, cellular stress-related gene expression alteration already at lower concentrations (0.1 mg/L) and demonstrating uptake potential in HDF. Overall, we demonstrate that PLA-NPs may induce toxicity, comparatively to PS-MPs. We wish to highlight the strong need to further investigate the related underlying molecular mechanisms, especially in the developing biota, to limit the high health risks related to PLA-based products.

Data availability

The data that support the findings of this study are available from the corresponding author (M.A.S.) upon reasonable request.

Received: 28 April 2025; Accepted: 24 September 2025
Published online: 31 October 2025

References

1. Lamparelli, E. P. et al. The other side of plastics: Bioplastic-Based nanoparticles for drug delivery systems in the brain. *Pharmaceutics* **15**, 2549 (2023).
2. Rillig, M. C., Kim, S. W. & Zhu, Y. G. The soil plastisphere. *Nat. Rev. Microbiol.* **22**, 64–74 (2024).
3. Waqas, M. et al. Marine plastic pollution detection and identification by using remote sensing-meta-analysis. *Mar. Pollut Bull.* **197**, 115746 (2023).
4. Andrady, A. L. Weathering and fragmentation of plastic debris in the ocean environment. *Mar. Pollut Bull.* **180**, 113761 (2022).
5. Song, Y. K. et al. Rapid production of Micro- and nanoplastics by fragmentation of expanded polystyrene exposed to sunlight. *Environ. Sci. Technol.* **54**, 11191–11200 (2020).
6. Xu, S. et al. Microplastics in aquatic environments: Occurrence, accumulation, and biological effects. *Sci. Total Environ.* **703**, 134699 (2020).
7. Jalaudin Basha, N. N., Hafiz, A., Osman, N. B. & Abu Bakar, N.F. Unveiling the noxious effect of polystyrene microplastics in aquatic ecosystems and their toxicological behavior on fishes and microalgae. *Front. Toxicol.* **5**, 1135081 (2023).
8. Bhagat, J., Zang, L., Nishimura, N. & Shimada, Y. Zebrafish: An emerging model to study microplastic and nanoplastic toxicity. *Sci. Total Environ.* **728**, 138707 (2020).
9. Garcia-Vazquez, E. et al. Towards a plastic-less planet. Gender and individual responsibility predict the effect of imagery nudges about marine (micro)plastic pollution on R-behavior intentions. *Mar. Pollut Bull.* **193**, 115157 (2023).
10. Knoblauch, D. & Mederake, L. Government policies combatting plastic pollution. *Curr. Opin. Toxicol.* **28**, 87–96 (2021).
11. Singhvi, M. S., Zinjarde, S. S. & Gokhale, D. V. Polylactic acid: synthesis and biomedical applications. *J. Appl. Microbiol.* **127**, 1612–1626 (2019).
12. de Albuquerque, T. L. et al. Polylactic acid production from biotechnological routes: A review. *Int. J. Biol. Macromol.* **186**, 933–951 (2021).
13. Santoro, A. et al. Plastamination: outcomes on the central nervous system and reproduction. *Curr. Neuropharmacol.* https://doi.org/10.2174/1570159X22666240216085947 (2024).
14. Liu, H. et al. Aging behavior of biodegradable polylactic acid microplastics accelerated by UV/H2O2 processes. *Chemosphere* **337**, 139360 (2023).
15. Weinstein, J. E., Dekle, J. L., Leads, R. R. & Hunter, R. A. Degradation of bio-based and biodegradable plastics in a salt marsh habitat: another potential source of microplastics in coastal waters. *Mar. Pollut Bull.* **160**, 111518 (2020).

16. Lyu, L. et al. The degradation of polylactic acid face mask components in different environments. *J. Environ. Manage.* **370**, 122731 (2024).
17. Klein, K. et al. Chemicals associated with biodegradable microplastic drive the toxicity to the freshwater oligochaete lumbriculus variegatus. *Aquat. Toxicol.* **231**, 105723 (2021).
18. Anderson, G. & Shenkar, N. Potential effects of biodegradable single-use items in the sea: polylactic acid (PLA) and solitary ascidians. *Environ. Pollut.* **268**, 115364 (2021).
19. Chagas, T. Q., Araújo, A. P. D. C. & Malafaia, G. Biomicroplastics versus conventional microplastics: an insight on the toxicity of these polymers in dragonfly larvae. *Sci. Total Environ.* **761**, 143231 (2021).
20. de Oliveira, J. P. J. et al. Behavioral and biochemical consequences of Danio rerio larvae exposure to polylactic acid bioplastic. *J. Hazard. Mater.* **404**, 124152 (2021).
21. Zhang, X. et al. Photolytic degradation elevated the toxicity of polylactic acid microplastics to developing zebrafish by triggering mitochondrial dysfunction and apoptosis. *J. Hazard. Mater.* **413**, 125321 (2021).
22. Duan, Z. et al. Diet preference of zebrafish (Danio rerio) for bio-based polylactic acid microplastics and induced intestinal damage and microbiota dysbiosis. *J. Hazard. Mater.* **429**, 128332 (2022).
23. Cheng, H. et al. Immunotoxic response of bio-based plastic on early life stage zebrafish (Danio rerio): A safe alternative to petroleum-based plastics? *J. Hazard. Mater.* **480**, 135846 (2024).
24. Shen, T. et al. Effects of microplastic (MP) exposure at environmentally relevant doses on the Structure, Function, and transcriptome of the kidney in mice. *Molecules* **28**, 7104 (2023).
25. La Pietra, A. et al. Polystyrene microplastics effects on zebrafish embryological development: comparison of two different sizes. *Environ. Toxicol. Pharmacol.* **106**, 104371 (2024).
26. De Marco, G. et al. Embryotoxicity of polystyrene microplastics in zebrafish Daniorerio. *Environ. Res.* **208**, 112552 (2022).
27. Lamparelli, E. P. et al. Lipid nano-vesicles for thyroid hormone encapsulation: A comparison between different fabrication technologies, drug loading, and an in vitro delivery to human tendon stem/progenitor cells in 2D and 3D culture. *Int. J. Pharm.* **624**, 122007 (2022).
28. Lamparelli, E. P. et al. PLA/PLGA nanocarriers fabricated by Microfluidics-Assisted nanoprecipitation and loaded with Rhodamine or gold can be efficiently used to track their cellular uptake and distribution. *Int. J. Pharm.* **667**, 124934 (2024).
29. Capparucci, F. et al. Evaluation of anaesthetic effect of commercial Basil ocimum Basilicum on zebrafish (Danio rerio) embryos. *Fishes* **7**, 318 (2022).
30. Scalia, F. et al. Muscle histopathological abnormalities in a patient with a CCT5 mutation predicted to affect the apical domain of the chaperonin subunit. *Front. Mol. Biosci.* **9**, 887336 (2022).
31. Choi, T. Y. et al. Zebrafish as an animal model for biomedical research. *Exp. Mol. Med.* **53**, 310–317 (2021).
32. Bellipanni, G. et al. Zebrafish as a model for the study of chaperonopathies. *J. Cell. Physiol.* **231**, 2107–2114 (2016).
33. Alberti, G. et al. Speeding up glioblastoma cancer research: highlighting the zebrafish xenograft model. *Int. J. Mol. Sci.* **25**, 5394 (2024).
34. Qiao, R. et al. Accumulation of different shapes of microplastics initiates intestinal injury and gut microbiota dysbiosis in the gut of zebrafish. *Chemosphere* **236**, 124334 (2019).
35. Russo, I. et al. The zebrafish model in dermatology: an update for clinicians. *Discov Oncol.* **13**, 48 (2022).
36. Delamare-Debouteville, J., Wood, D. & Barnes, A. C. Response and function of cutaneous mucosal and serum antibodies in barramundi (Lates calcarifer) acclimated in seawater and freshwater. *Fish. Shellfish Immunol.* **21**, 92–101 (2006).
37. Kimmel, C. B. et al. Stages of embryonic development of the zebrafish. *Dev. Dyn.* **203**, 253–310 (1995).
38. Tallec, K. et al. Surface functionalization determines behavior of nanoplastic solutions in model aquatic environments. *Chemosphere* **225**, 639–646 (2019).
39. Shen, M. et al. Recent advances in toxicological research of nanoplastics in the environment: A review. *Environ. Pollut.* **252**, 511–521 (2019).
40. Chandraharan, E., Ghi, T., Fieni, S. & Jia, Y. J. Optimizing the management of acute, prolonged decelerations and fetal bradycardia based on the Understanding of fetal pathophysiology. *Am. J. Obstet. Gynecol.* **228**, 645–656 (2023).
41. da Silva, D. et al. Biocompatibility, biodegradation and excretion of polylactic acid (PLA) in medical implants and theranostic systems. *Chem. Eng. J.* **340**, 9–14 (2018).
42. Wang, M. et al. Oligomer nanoparticle release from polylactic acid plastics catalysed by gut enzymes triggers acute inflammation. *Nat. Nanotechnol.* **18**, 403–411 (2023).
43. Duan, Z. et al. Plastic food? Energy compensation of zebrafish (Danio rerio) after long-term exposure to polylactic acid biomicroplastics. *J. Hazard. Mater.* **466**, 133604 (2024).
44. Castañeda-Rodríguez, S. et al. Recent advances in modified Poly (lactic acid) as tissue engineering materials. *J. Biol. Eng.* **17**, 21 (2023).
45. Kozal, J. S. et al. Uptake, tissue distribution, and toxicity of polystyrene nanoparticles in developing zebrafish (Danio rerio). *Aquat. Toxicol.* **194**, 185–194 (2018).
46. Leyden, C. et al. Efficacy of Tricaine (MS-222) and hypothermia as anesthetic agents for blocking sensorimotor responses in larval zebrafish. *Front. Vet. Sci.* **9**, 864573 (2022).
47. Craig, M. P., Gilday, S. D. & Hove, J. R. Dose-dependent effects of chemical immobilization on the heart rate of embryonic zebrafish. *Lab. Anim. (NY).* **35**, 41–47 (2006).
48. Pitt, J. A. et al. Uptake, tissue distribution, and toxicity of polystyrene nanoparticles in developing zebrafish (Danio rerio). *Aquat. Toxicol.* **194**, 185–194 (2018).
49. Zhu, X. et al. Micro- and nanoplastics: A new cardiovascular risk factor? *Environ. Int.* **171**, 107662 (2023).
50. Yan, J. et al. Toxic vascular effects of polystyrene microplastic exposure. *Sci. Total Environ.* **905**, 167215 (2023).
51. Zheng, F. et al. Redox toxicology of environmental chemicals causing oxidative stress. *Redox Biol.* **34**, 101475 (2020).
52. Kadac-Czapska, K., Ośko, J., Knez, E. & Grembecka, M. Microplastics and oxidative Stress-Current problems and prospects. *Antioxid. (Basel).* **13**, 579 (2024).
53. Pickering, A. M., Vojtovich, L., Tower, J. A. & Davies, K. J. Oxidative stress adaptation with acute, chronic, and repeated stress. *Free Radic Biol. Med.* **55**, 109–118 (2013).
54. Lushchak, V. I. & Storey, K. B. Oxidative stress concept updated: Definitions, classifications, and regulatory pathways implicated. *EXCLI J.* **20**, 956–967 (2021).
55. Holowiecki, A., O'Shields, B. & Jenny, M. J. Characterization of Heme Oxygenase and biliverdin reductase gene expression in zebrafish (Danio rerio): basal expression and response to pro-oxidant exposures. *Toxicol. Appl. Pharmacol.* **356**, 98 (2018).
56. Ding, P. et al. Photoaged microplastics induce neurotoxicity via oxidative stress and abnormal neurotransmission in zebrafish larvae (Danio rerio). *Sci. Total Environ.* **881**, 163480 (2023).
57. Li, R. et al. Toxic effect of chronic exposure to polyethylene nano/microplastics on oxidative stress, neurotoxicity and gut microbiota of adult zebrafish (Danio rerio). *Chemosphere* **339**, 139774 (2023).
58. Félix, L., Carreira, P. & Peixoto, F. Effects of chronic exposure of naturally weathered microplastics on oxidative stress level, behaviour, and mitochondrial function of adult zebrafish (Danio rerio). *Chemosphere* **310**, 136895 (2023).
59. Hu, M. & Palić, D. Micro- and nano-plastics activation of oxidative and inflammatory adverse outcome pathways. *Redox Biol.* **37**, 101620 (2020).

60. Lam, S. H. et al. Development and maturation of the immune system in zebrafish, Danio rerio: a gene expression profiling, in situ hybridization and immunological study. *Dev. Comp. Immunol.* **28**, 9–28 (2004).
61. Solleiro-Villavicencio, H. & Rivas-Arancibia, S. Effect of chronic oxidative stress on neuroinflammatory response mediated by CD4 + T cells in neurodegenerative diseases. *Front. Cell. Neurosci.* **12**, 114 (2018).
62. Rehman, A. et al. Nanoplastic contamination: impact on zebrafish liver metabolism and implications for aquatic environmental health. *Environ. Int.* **187**, 108713 (2024).
63. Xiong, G. et al. Enhanced hepatotoxicity in zebrafish due to co-exposure of microplastics and sulfamethoxazole: insights into ROS-mediated MAPK signaling pathway regulation. *Ecotoxicol. Environ. Saf.* **278**, 116415 (2024).
64. Savuca, A. et al. Do microplastics have neurological implications in relation to schizophrenia zebrafish models? A brain Immunohistochemistry, neurotoxicity Assessment, and oxidative stress analysis. *Int. J. Mol. Sci.* **25**, 8331 (2024).
65. Cao, X. et al. Nanoplastic exposure mediates neurodevelopmental toxicity by activating the oxidative stress response in zebrafish (Danio rerio). *ACS Omega*. **9**, 16508–16518 (2024).
66. Wang, X. et al. Microplastic-mediated new mechanism of liver damage: from the perspective of the gut-liver axis. *Sci. Total Environ.* **919**, 170962 (2024).
67. Nihart, A. J. et al. Bioaccumulation of microplastics in decedent human brains. *Nat. Med.* https://doi.org/10.1038/s41591-025-03675-x (2025).
68. Lin, W. et al. Polystyrene microplastics enhance the microcystin-LR-induced gonadal damage and reproductive endocrine disruption in zebrafish. *Sci. Total Environ.* **876**, 162664 (2023).
69. Rong, W. et al. Effects of combined exposure to polystyrene microplastics and 17α-Methyltestosterone on the reproductive system of zebrafish. *Theriogenology* **215**, 158–169 (2024).
70. Zha, H. et al. Polylactic acid micro/nanoplastic-induced hepatotoxicity: investigating food and air sources via multi-omics. *Environ. Sci. Ecotechnol.* **21**, 100428 (2024).
71. Teng, M. et al. Vitamin D modulation of brain-gut-virome disorder caused by polystyrene nanoplastics exposure in zebrafish (Danio rerio). *Microbiome* **11**, 266 (2023).
72. Huang, J. N. et al. Integrated response of growth, antioxidant defense and isotopic composition to microplastics in juvenile Guppy (Poecilia reticulata). *J. Hazard. Mater.* **399**, 123044 (2020).
73. Ali, N. et al. The potential impacts of micro-and-nano plastics on various organ systems in humans. *EBioMedicine* **99**, 104901 (2024).
74. Sabourian, P. et al. Effect of Physico-Chemical properties of nanoparticles on their intracellular uptake. *Int. J. Mol. Sci.* **21**, 8019 (2020).

Acknowledgements

This work was funded by the European Union – Next Generation EU" M4.C2. component, investment 1.1, "Fund for the National Research Program and Projects of Relevant National Interest" – PRIN-PNRR2022: Identification code P2022AA47Y_003, CUP: B53D23032060001 - ERC sector ERC-LS9 - project code U-GOV PRJ-1538, Project title: Poly(Lactic Acid) plastics contamination (PLASTAMINATION): organ injuries and underlying molecular mechanisms.

Author contributions

Conceptualization, F.S.; F.C.; A.S. and M.A.S.; validation, F. Cappello and A.S.; formal analysis, F.S.; C.F.; M.M.; E.P.L.; L.L. and M.A.S.; methodology, F.S.; F.C.; M.D.A.; F.R.; M.M.; E.P.L.; S.G.; R.F. and M.A.S.; resources, L.L.; C.I.; F.M.; G.D.; A.S.; F. Cappello and M.A.S.; data curation, F.S.; F.C. and M.A.S; , writing—original draft preparation, F.S.; M.D.A. and M.A.S.; writing—review and editing, F.S.; F.C.; M.M.; L.L.; A.M.G.; F.B. and M.A.S.; funding acquisition, A.S. and F. Cappello. All authors have read and agreed to the published version of the manuscript.

Declarations

Competing interests

The authors declare no competing interests.

Additional information

Supplementary Information The online version contains supplementary material available at https://doi.org/10.1038/s41598-025-21849-y.

Correspondence and requests for materials should be addressed to M.A.S.